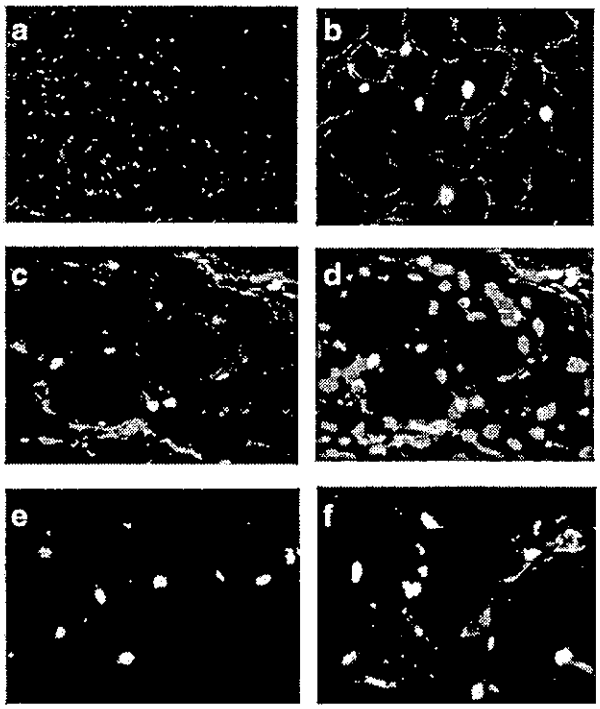

Figure 2 The cellular localization of transfected ODN. FITC-labeled ODN accumulated in the interstitial cells 10 min after retrograde transfection by electroporation (a). To examine the cellular localization of the transfected ODN, rabbit polyclonal anti-laminin antibodies and Texas red-conjugated anti-rabbit IgG were used to stain the basement membrane (b). FITC (green)-positive cells were observed outside the basement membrane (red). To identify the transfected cells, the antibodies for RECA-1 (c, d), ED1 (e), and ER-TR7 (f) were used. Transfected interstitial cells were not coincident with endothelial cells (c, d) or macrophages (e), but were shown to be fibroblast-like cells (f). In addition, FITC-labeled ODN were introduced into the nuclei (blue) 10 min after transfection (d).

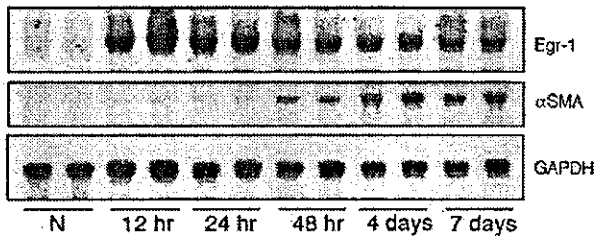

Figure 3 Egr-1 and αSMA mRNA expression after ureteral obstruction. Each lane represents RNA (20 μg) from the cortex of normal kidney (N) or obstructed kidney 12, 24 and 48 h and 4 and 7 days after ureteral ligation. The top panel shows the Egr-1 mRNA, and middle panel shows the αSMA mRNA. The bottom panel represents the GAPDH mRNA.

enhanced expression of αSMA was observed in the interstitial area of untreated or SCR-treated obstructed kidneys. However, αSMA induction was weak in the ED5-treated obstructed kidneys (Figure 5).

Effect on interstitial fibrosis

To determine the effect on the interstitial fibrotic changes in obstructed kidneys, histological analysis was performed using Masson's trichrome staining (Figure 6a). The area of the fibrotic lesion of the cortical interstitium was

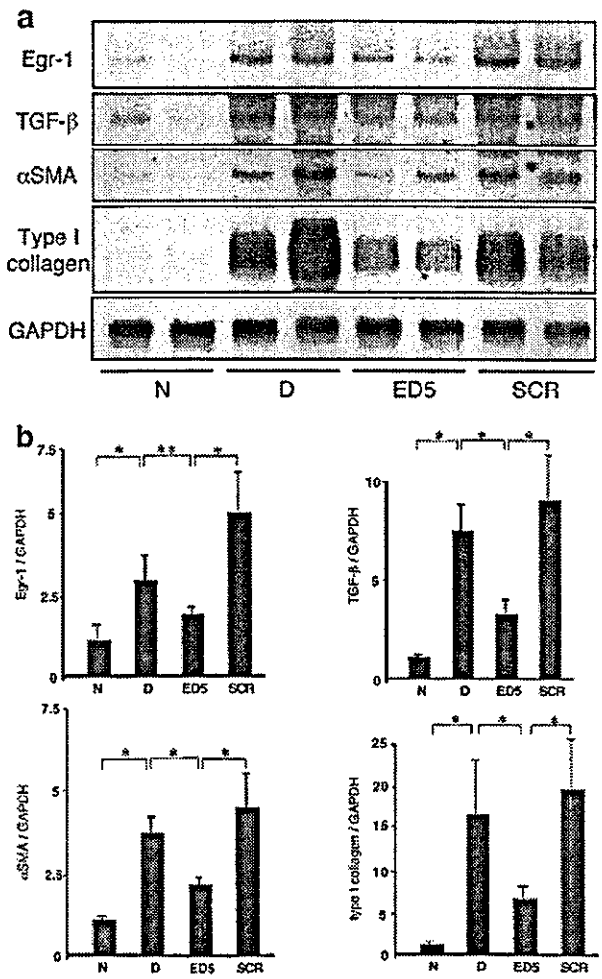

Figure 4 Inhibition of Egr-1, TGF-β1, αSMA and type I collagen mRNA expression in obstructed kidneys by the DNA enzyme, ED5. (a) Each lane shows representative mRNA from the cortex of normal kidney (N), untreated obstructed kidney (D), SCR-treated obstructed kidney (SCR), and ED5-treated obstructed kidney (ED5). Northern blot was probed for Egr-1, TGF-β1, αSMA, type I collagen or GAPDH. (b) The band density in three experiments expressed as the mean ± s.d. is illustrated (, $P < 0.01$; **, $P < 0.05$).*

determined in the sections stained light blue (Figure 6b). Untreated obstructed kidneys for 7 days showed an expanded interstitium compared with normal kidney. SCR-treated obstructed kidneys exhibited increased tubular dilation, with a marked expansion of the interstitium. In contrast, ED5-treated obstructed kidneys showed a minimal interstitial expansion, although they exhibited the same extent of tubular dilation. There was no difference in the severity of interstitial fibrosis between untreated obstructed kidneys and SCR-treated kidneys. In contrast, the area of interstitial fibrosis was significantly suppressed in ED5-treated obstructed kidneys compared with untreated or SCR-treated obstructed kidneys ($P < 0.01$) (Figure 6b).

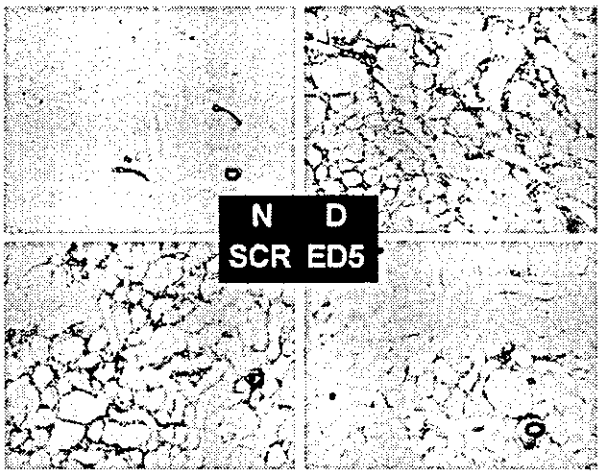

Figure 5 Inhibition of interstitial expression of αSMA by ED5. Representative photomicrographs show the immunohistochemical staining for αSMA in normal kidney (N), untreated obstructed kidney (D), SCR-treated obstructed kidney (SCR), and ED5-treated obstructed kidney (ED5) (×200).

Discussion

In the present study we demonstrated that introduction of DNA enzyme for Egr-1 into interstitial fibroblasts by electroporation-mediated gene transfer could suppress Egr-1 expression and thereby inhibit consequent interstitial fibrosis in obstructed kidneys. Despite various approaches and techniques, few successful studies have been reported concerning *in vivo* transfection targeting interstitial fibroblasts, which have been highlighted as the source of increased extracellular matrix synthesis.[3] In our previous studies, we showed that retrograde transfection via the ureter using the AVE-type HVJ–liposome method enabled selective DNA introduction into interstitial fibroblasts.[26] We suggested that retrogradely infused DNA solution could enter into the interstitial area by slipping through between papilla epithelial cells, and thereafter distribute diffusely in the cortical interstitial spaces.[26] More recently, we reported that *in vivo* electroporation, DNA injection via renal artery followed by application of electric fields, provides an efficient approach for glomerulus-targeted gene transfer.[28] In addition, *in vivo* electroporation with intra-renal-arterial DNA injection was more effective than the HVJ–liposome method.[28] By means of these innovative gene transfer methods, we demonstrated here that retrograde DNA injection via the ureter followed by electroporation resulted in interstitial fibroblast-targeted gene transfer. Its advantages, compared with viral vectors, are that it is simple, inexpensive and less harmful.

A number of cytokines, vasoactive compounds, chemoattractant molecules, and growth factors are involved in the development of interstitial fibrosis.[3] The plasticity of resident fibroblasts to assume a myofibroblastic alteration, which can be identified by αSMA expression, is one of the most important events associated with increased matrix accumulation.[3–6] TGF-β[24,25] and PDGF-BB[23,30] are two growth factors that can transform fibroblasts. We have especially highlighted interstitial cells as a major source of TGF-β1, and showed that the

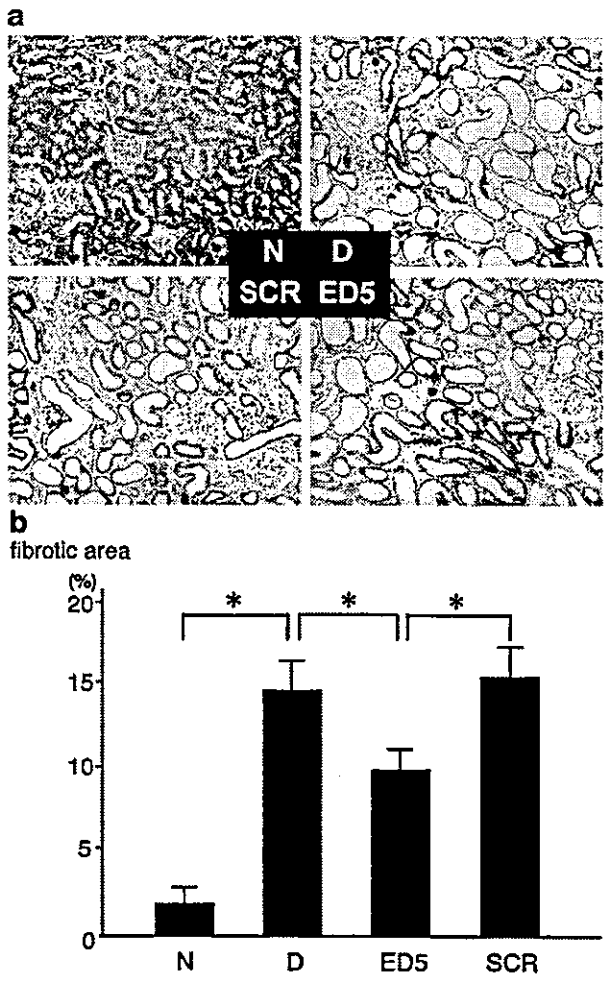

Figure 6 Inhibition of interstitial fibrosis by ED5. (a) Representative photomicrographs show the Masson's trichrome staining in normal kidney (N), untreated obstructed kidney (D), SCR-treated obstructed kidney (SCR), and ED5-treated obstructed kidney (ED5) (×200). (b) The area of interstitial fibrosis is summarized.

inhibition of interstitial TGF-β1 expression resulted in the suppression of interstitial fibrosis.[27] Here, we demonstrated that inhibition of interstitial Egr-1 expression suppressed TGF-β1 expression, and thereby ameliorated interstitial fibrosis. Taken together with our previous findings,[27] interstitial fibroblasts play an important role in the formation of interstitial fibrosis.

Egr-1 was reported to influence the transcription of a diverse set of genes. Egr-1 has been implicated in the induced expression of growth factors such as TGF-β,[16] PDGF-B,[20] and basic fibroblast growth factor.[17] Cytokines, such as TNF-α,[31] and adhesion molecules, such as ICAM-1[21] can be affected. Recently, activation of Egr-1 was shown to function as a master switch activated by ischemia to trigger expression of pivotal regulators of inflammation, coagulation and vascular hyperpermeability.[32] Deletion of the gene encoding Egr-1 strikingly diminished expression of these mediators of vascular injury in a murine model of lung ischemia/reperfusion injury, and enhanced animal survival and organ function. We found the elevated Egr-1 expression immediately

after ureteral obstruction before the expression of a set of fibrogenic genes. We showed that inhibition of Egr-1 by ED5 ameliorated TGF-β1, αSMA, and type I collagen expression. In addition, we observed the suppression of PDGF-B mRNA expression in ED5-transfected obstructed kidneys by RT-PCR (data not shown). These findings suggest that Egr-1-mediated gene transcription plays a key role in orchestrating the functional characteristics of tubulointerstitial fibrosis, and that inhibition of Egr-1 may suppress the above gene's expression, and thereby manipulate the interstitial fibrosis.

To inhibit the gene expression by cleavage of the target mRNA, antisense ODN and ribozymes have been adopted.[33,34] Since the antisense mechanism is based on the hydrolysis of the RNA-DNA duplex by RNase H,[35] the effect of antisense may be transient. Ribozymes are catalytic RNA molecules that selectively bind to an RNA substrate and cleave phosphodiester bonds. However, the utility of ribozymes has been limited by their susceptibility to degradation by RNase. Recently, a new generation of catalytic nucleic acids composed of DNA, named DNA enzyme, was developed.[29,36] These DNA enzymes can potentially cleave RNA at any purine-pyrimidine junction and offer greater substrate specificity than hammerhead ribozymes. We demonstrated that the serum-stimulated Egr-1 expression was specifically blocked by treatment with the DNA enzyme for Egr-1 in cultured NRK cells. In addition, the introduction of DNA enzyme into interstitial fibroblasts suppressed the elevated Egr-1 expression in obstructed kidneys. It was reported that the antisense effect was similar to DNA enzyme only if the concentration of antisense ODN was increased by 600% of the DNA enzyme.[29] For resistance to 3'-to-5' exonuclease digestion, the 3' terminus of the DNA enzyme was capped with an inverted 3'-3'-linked thymidine. Therefore, the DNA enzyme appears to remain more stable than ribozymes or antisense ODN. In addition, phosphorothioate-modified ODN may hamper cellular function, because an additional negative charge on the ODN increases binding affinity for intracellular proteins.

In conclusion, the findings of the present study demonstrated that Egr-1 plays an important part in coordinating phenotypic alteration and the development of interstitial fibrosis. DNA injection via the ureter followed by electroporation could represent a powerful investigative and potentially therapeutic tool *in vivo*. In addition the molecular intervention by DNA enzyme may be a useful strategy for interstitial renal diseases.

Materials and methods

Cell culture

NRK cells, a fibroblast cell line derived from rat kidney, were a generous gift from the Japanese Cancer Research Resources Bank. Cells were grown in Dulbecco's modified Eagle's medium (DMEM; Sigma, St Louis, MO, USA) containing 10% FCS equilibrated with 5% CO^2–95% air at 37°C. The cells at passages 35 to 40 were used.

Design of DNA enzyme

Sequences of the DNA enzyme for rat Egr-1 (ED5)[29] used in the present study were 5'-CCGCTGCCA GGCTAGCTACAACGACCCGGACGTT-3' (3' thymidine inverted; italic, catalytic domain; underlined) (Bex, Tokyo, Japan). ED5 has two nine-nucleotide arms flanking the 15-nucleotide catalytic domain (underlined), which was designed to target the translational site AUG in rat Egr-1 mRNA. For resistance to 3'-to-5' exonuclease digestion, the 3' terminus of the molecule was capped with an inverted 3'-3'-linked thymidine (italics). The nucleotide sequence in each arm of ED5 was scrambled without altering the catalytic domain (SCR). SCR sequences were 5'-GCCAGCCGCGGCTAGCTACAACGA TGGCTCAACT (3' thymidine inverted; italics, catalytic domain; underlined). ED5 was reported to cleave Egr-1 mRNA specifically.[29]

Egr-1 mRNA expression on NRK cells

To examine the Egr-1 mRNA expression on NRK cells, Northern blot analysis was performed. NRK cells grown to subconfluency in 100-mm dishes with DMEM containing 10% FCS were made quiescent in 0.5% FCS for 48 h. Then, the cells were incubated in a medium with 0.5, 2, 5 or 10% of FCS for 60 min to examine the effect of the FCS concentration on Egr-1 mRNA expression. To examine the time course of mRNA expressions after stimulation by FCS, NRK cells were incubated with 5% FCS for 30, 60 or 120 min. After stimulation, the cells were washed three times with cold phosphate-buffered saline (PBS) and scraped and suspended with 1 ml of acid-guanidium thiocyanate-phenol-chloroform extraction (Trizol reagent; Life Technologies, Gaithersburg, MD, USA).[37] Twenty micrograms of extracted total RNA were separated on a 1% agarose formaldehyde gel and transferred to a nylon membrane (Hybond-N+; Amersham, Boston, MA, USA) by capillary elution. Rat Egr-1 cDNA[12] was labeled by the random priming method using [α-^{32}P] dCTP (3000 Ci/mmol, Amersham). Hybridization was carried out at 42°C overnight in 50% formamide, 5 × SSC, 0.1% SDS, 20 mM sodium phosphate buffer, 10 × Denhardt's solution and 200 μg/ml salmon sperm DNA. The membrane was washed twice at 55°C and 60°C with 1 × SSC, 0.1% SDS and subjected to autoradiography.

Effects of the DNA enzyme on Egr-1 expression in vitro

Subconfluent (50%) NRK cells were incubated in a medium with ED5 or SCR (1 or 5 μM), and grown to 90% confluency. Treated NRK cells were made quiescent for 48 h in 0.5% FCS medium, and then stimulated with serum. After stimulation with 5% FCS for 60 min, total RNA was extracted for Northern blot analysis as above. For Western blot analysis, treated NRK cells were stimulated with 5% FCS for 120 min, and the cells were washed three times with cold PBS and scraped and suspended with 200 μl of protein extract solution (1% Triton X-100, 50 mM Tris-HCl, pH 7.5 150 mM NaCl, 2 mM Na3VPO4, 5 mM EDTA, 2 μg/ml aprotinin, 0.7 μg/ml pepstatin, 0.1 mg/ml Pefabloc SC, and 100 mM NaF). The extracted protein solution containing 40 μg of proteins was separated by electrophoresis through 7.5% sodium dodecyl sulfate-polyacrylamide gel electrophoresis (SDS-PAGE). They were then electrotransferred on to nitrocellulose membranes. Egr-1 proteins were detected with anti-Egr-1 antibody (588; Santa Cruz Biotechnology, Santa Cruz, CA, USA) at a 1:1000 dilution by standard procedures and anti-rabbit antibody conjugated to horseradish peroxidase (Santa Cruz) at a 1:1000 dilution, and visualized using an enhanced chemiluminescence kit (NEN Life Science Products, Boston, MA, USA).

Electroporation-mediated retrograde gene transfer into interstitial cells

To develop a new gene transfer system targeting interstitial fibroblasts, we first transfected FITC-labeled ODN using an electroporation-mediated retrograde gene transfer method. Six-week-old male Sprague–Dawley rats (n = 4) weighing approximately 150 g (Japan SLC, Hamamatsu, Japan) were anesthetized by intraperitoneal injection of pentobarbital (50 mg/kg), and the left kidney and ureter were surgically exposed. FITC-labeled ODN (50 μg) in 500 μl of balanced salt solution (BSS) were injected slowly into the left kidney via the ureter using a 30-gauge needle with clamping of the left renal vein. Immediately after injection, the ureter was obstructed by silk thread and the left kidney was sandwiched with the tweezer-type oval-shaped stainless steel electrode. Then square wave electric pulses (six times) at 75 V were delivered. Ten minutes after transfection, the kidneys were perfused with PBS and samples of the cortex were frozen by liquid nitrogen.

Electric pulse delivered and electrodes

Electric pulses were delivered using an electric pulse generator (Electro Square Porator T820; BTX, San Diego, CA, USA) connected to a switch box (MBX-4BTX) and monitored using a graphic pulse analyzer (Optimizer 500; BTX). The shape of the pulse was a square wave and the voltage remained constant during the pulse duration. Three pulses of the indicated voltage followed by three more pulses of the opposite polarity were administrated to the kidney. Intrapulse delay was 1 s and the duration of the pulse was fixed at 99 ms.

Experimental design

To determine the therapeutic effect of the DNA enzyme on interstitial fibrosis, we employed a unilateral ureteral obstruction model. Before the therapeutic examination, we studied the expression of Egr-1 and αSMA after induction of the ureteral obstruction. All procedures were handled in a humane fashion in accordance with the guidelines of the Animal Committee of Osaka University. Six-week-old male SD rats were anesthetized by intraperitoneal injection of pentobarbital (50 mg/kg) and the left proximal ureter was ligated with silk thread. For RNA extraction, obstructed kidneys were harvested at 12, 24, 48 h and 4 and 7 days after ureteral ligation (n = 4 for each group). In the next experiment, SD rats were anesthetized by intraperitoneal injection of pentobarbital, and the left kidney and ureter were surgically exposed by a mid-line incision. ED5 or SCR (200 μg) in 500 μl of BSS was injected into left kidney via ureter using a 30-gauge needle with clamping of the left renal vein. Immediately after injection of the solution, the ureter was obstructed by silk thread and the kidney was sandwiched with tweezer-type oval-shaped stainless electrode. Square wave electric pulses at 75 V (six times) were delivered. On day 7, the kidneys were perfused with cold autoclaved PBS, and samples of the cortex were taken for RNA preparations and histology (n = 6 for each group). Tissues for RNA were frozen using liquid nitrogen and homogenized with acid-guanidium thiocyanate-phenol-chloroform extraction. Tissues for light microscopy were fixed with 4% paraformaldehyde overnight and dehydrated through a graded ethanol series and embedded in paraffin. Histological sections (2 μm) of the kidneys were stained by Masson's trichrome method. Tissues for immunohistochemistry were fixed in methyl Carnoy's solution and sections (4 μm) were stained with αSMA.

The area of the interstitial fibrosis stained in blue by Masson's trichrome staining was measured by computerized image analysis using the Mac SCOPE programs. In brief, randomly selected cortical fields at ×200 magnification (n = 6) from each rat were photographed. The captured image was converted and modified to eliminate the area occupied by glomeruli and tubular lumena. The region of blue staining was automatically measured with determined threshold settings. The results were expressed as the percent area of interstitial fibrosis.

Immunofluorescence

To identify the cells where FITC-labeled ODN were introduced, the transfected kidneys were stained with the antibodies to rat laminin (a marker for tubular basement membrane; Monosan, Amuden, The Netherlands) and the mouse monoclonal antibody to rat RECA-1 (a marker for endothelial cells; Cosmo Bio, Tokyo, Japan), the monoclonal antibody ED1 (a marker for macrophages; Serotec, Oxford, UK), and ER-TR7 (a marker for fibroblasts; Biogenesis, New Fields, UK).[38] Four micrometer slices of frozen sections were incubated with these first antibodies for 1 h at room temperature followed by the incubation with Texas red-conjugated second antibodies for 30 min at room temperature. The green fluorescence of FITC and the red fluorescence of Texas red were taken by photomicrography on the same film by double exposure. Transfected kidney specimens labeled with anti-RECA-1 antibody were also stained with 0.1 μM of the nucleic acid dye 4′6′-diamino-2-phenylindole (DAPI; Molecular Probes, Eugene, OR, USA).

Immunohistochemistry

To examine the expression of αSMA, immunohistochemical staining was performed on tissues fixed in methyl Carnoy's solution. Tissue sections were preincubated with horse serum diluted 1:20 with PBS for 30 min to block the nonspecific staining, and then incubated with mouse IgG anti-αSMA monoclonal antibodies (Immunotech, Marseilles, France) for 60 min at room temperature. The endogenous peroxidase activity in tissue sections was blocked by incubating in methanol with 0.3% hydroxyoxidase for 30 min. The sections were then processed using an avidin-biotinylated peroxidase complex method (Vectastain ABC kit; Vector Laboratories, Burlingame, CA, USA) with diaminobenzidine as the chromogen. The sections were counterstained with methyl green.

Northern blot analysis

To examine the effect of the DNA enzyme on the level of Egr-1,[12] TGF-β1, αSMA, and type I collagen, Northern blot analysis was performed with cortical RNA extracted from untransfected or transfected obstructed kidneys. The kidneys were perfused with cold autoclaved PBS and the tissues of the cortex were removed, and snap-frozen in liquid nitrogen. The renal cortex was homogenized with a Polytron homogenizer (Kinematica, Switzerland) in Trizol reagent. For Northern analysis, rat Egr-1, TGF-β1, type I collagen and glyceraldehyde-3-phosphate dehydrogenase (GAPDH) cDNA were labeled by the random priming method using [α-^{32}P] dCTP (3000 Ci/mmol,

Amersham) and hybridization was carried out using the same procedure in the *in vitro* study reported above. The membrane which hybridized with Egr-1, TGF-β1 and GAPDH were washed, twice at 50°C and twice at 55°C in 1 × SSC, 0.1% SDS, and once at 55°C in 0.5 × SSC, 0.1% SDS. The membrane hybridized with type I collagen was washed twice at 50°C and twice at 55°C in 0.1 × SSC 0.1% SDS and subjected to autoradiography.

αSMA cDNA was labeled using [γ-^{32}P] ATP and hybridized at 42°C overnight in 50% formamide, 5 × SSC, 0.1% SDS, 20 mM sodium phosphate buffer, 10 × Denhardt's solution and 200 μg/ml salmon sperm DNA. The membrane was washed twice at 55°C in 5 × SSC, 0.1% SDS and twice at 55°C in 1 × SSC, 0.1% SDS and subjected to autoradiography.

Autoradiographs were obtained and the density of each band was quantified using the laser densitometry (Scanning Imager; Molecular Dynamics, Sunnyvale, CA, USA). These experiments were repeated three times and the density of each band relative to that of GAPDH was calculated.

Statistical analysis

All values are expressed as means ± s.d. Statistical significance was evaluated using the one-way analysis of variance (ANOVA).

References

1 Risdon R, Sloper J, de Vardener H. Relationship between renal function and histologic changes found in renal-biopsy specimens from patients with persistent glomerulonephritis. *Lancet* 1968; 2: 363–366.
2 Schainuck LI, Striker GE, Cutler RE, Benditt EP. Structural-functional correlations in renal disease. II. The correlations. *Hum Pathol* 1970; 1: 631–641.
3 Eddy AA. Molecular insights into renal interstitial fibrosis. *J Am Soc Nephrol* 1996; 7: 2495–2508.
4 Alpers C, Hudkins K, Floege J, Johnson R. Human renal cortical interstitial cells with some features of smooth muscle cells participate in tubulointerstitial and crescentic glomerular injury. *J Am Soc Nephrol* 1994; 5: 201–210.
5 Diamond JR, Kees FD, Ricardo SD, Pruznak A, Eufemio M. Early and persistent up-regulated expression of renal cortical osteopontin in experimental hydronephrosis. *Am J Pathol* 1996; 146: 1455–1466.
6 Kliem V *et al*. Mechanisms involved in the pathogenesis of tubulointerstitial fibrosis in 5/6-nephrectomized rats. *Kidney Int* 1996; 49: 666–678.
7 Sappino A, Schurch W, Gabbiani G. Differentiation repertoire of fibroblastic cells: expression of cytoskeletal proteins as marker of phenotypic modulations. *Lab Invest* 1990; 63: 144–161.
8 Skalli O *et al*. A monoclonal antibody against alpha-smooth muscle actin: a new probe for smooth muscle differentiation. *J Cell Biol* 1986; 103: 2787–2796.
9 Skalli O, Vandekerckhove J, Gabbiani G. Actin-isoform pattern as a marker of normal or pathological smooth-muscle and fibroblastic tissues. *Differentiation* 1987; 33: 232–238.
10 Vandekerckhove J, Weber K. At least six different actins are expressed in a higher mammal: an analysis based on the amino acid sequence of the amino-terminal tryptic peptide. *J Mol Biol* 1978; 33: 783–802.
11 Hewitson T, Becker G. Interstitial myofibroblasts in IgA glomerulonephritis. *Am J Nephrol* 1995; 15: 111–117.
12 Rupprecht H *et al*. Expression of the transcriptional regulator Egr-1 in experimental glomerulonephritis: requirement for mesangial cell proliferation. *Kidney Int* 1997; 51: 694–702.
13 Gashler A, Sukhatme V. Early growth response protein 1 (Egr-1): prototype of a zinc-finger family of transcription factors. *Prog Nucleic Acid Res Mol Biol* 1995; 50: 191–224.
14 Khachigian L, Collins T. Inducible expression of Egr-1-dependent genes: a paradigm of transcriptional activation in vascular endothelium. *Circ Res* 1997; 81: 457–461.
15 Silverman E, Collins T. Pathways of Egr-1-mediated gene transcription in vascular biology. *Am J Pathol* 1999; 154: 665–670.
16 Kim S *et al*. Promoter sequences of the human transforming growth factor-β1 gene responsive to transforming growth factor-β1 autoinduction. *J Biol Chem* 1989; 264: 7041–7045.
17 Biesiada E, Razandi M, Levin E. Egr-1 activates basic fibroblast growth factor transcription. Mechanistic implications for astrocyte proliferation. *J Biol Chem* 1996; 271: 18576–18581.
18 Khachigian L, Williams A, Collins T. Interplay of Sp1 and Egr-1 in the proximal platelet-derived growth factor A-chain promoter in cultured vascular endothelial cells. *J Biol Chem* 1995; 270: 27679–27686.
19 Silverman E, Khachigian L, Lindner V, Williams A, Collins T. Inducible PDGF A-chain transcription in smooth muscle cells is mediated by Egr-1 displacement of Sp1 and Sp3. *Am J Physiol* 1997; 273: H1415–H1426.
20 Khachigian L, Lindner L, Williams A, Collins T. Egr-1-induced endothelial gene expression: a common theme in vascular injury. *Science* 1996; 271: 1427–1431.
21 Maltzman J, Carmen J, Monroe J. Transcriptional regulation of the ICAM-1 gene in antigen receptor- and phorbol ester-stimulated B lymphocytes: role for transcription factor EGR1. *J Exp Med* 1996; 183: 1747–1759.
22 Maltzman J, Carman J, Monroe J. Role of EGR1 in regulation of stimulus-dependent CD44 transcription in B lymphocytes. *Mol Cell Biol* 1996; 16: 2283–2294.
23 Alpers CE *et al*. Developmental patterns of PDGF B-chain PDGF-receptor and alpha-actin expression in human glomerulogenesis. *Kidney Int* 1992; 42: 390–399.
24 Border W, Noble N. Transforming growth factor in tissue fibrosis. *N Engl J Med* 1994; 331: 1286–1292.
25 Yamamoto T, Noble NA, Miller DE, Border WA. Sustained expression of TGF-beta 1 underlies development of progressive kidney fibrosis. *Kidney Int* 1994; 45: 916–927.
26 Tsujie M *et al*. Gene transfer targeting interstitial fibroblasts by the artificial viral envelope type hemagglutinating virus of Japan liposome method. *Kidney Int* 2000; 57: 1973–1980.
27 Isaka Y *et al*. Introduction of transforming growth factor-beta 1 antisense oligodeoxynucleotides into renal interstitial fibroblasts blocks interstitial fibrosis in unilateral ureteral obstruction. *Kidney Int* 2000; 58: 1885–1892.
28 Tsujie M, Isaka Y, Nakamura H, Imai E, Hori M. Electroporation mediated gene transfer that targets glomeruli. *J Am Soc Nephrol* 2001; 12: 949–954.
29 Santiago F *et al*. New DNA enzyme targeting Egr-1 mRNA inhibits vascular smooth muscle proliferation and regrowth after injury. *Nat Med* 1999; 5: 1264–1269.
30 Alpers CE, Hudkins KL, Floege J, Johnson RJ. Human renal cortical interstitial cells with some features of smooth muscle cells participate in tubulointerstitial and crescentic glomerular injury. *J Am Soc Nephrol* 1994; 5: 201–209.
31 Kramer B *et al*. Characterization of a Krox-24/Egr-1-responsive element in the human tumor necrosis factor promoter. *Biochim Biophys Acta* 1994; 1219: 413–421.
32 Yan S *et al*. Egr-1, a master switch coordinating upregulation of divergent gene families underlying ischemic stress. *Nat Med* 2000; 6: 1355–1361.
33 Imai E, Isaka Y. Strategies of gene transfer to the kidney. *Kidney Int* 1998; 53: 264–272.
34 Fine LG. Gene transfer into the kidney: promise for unravelling disease mechanisms, limitations for human gene therapy. *Kidney Int* 1996; 49: 612–619.
35 Wanger R. Gene inhibition using antisense oligodeoxynucleotides. *Nature* 1994; 372: 333–335.
36 Santoro SW, Joyce GF. A general purpose RNA-cleaving DNA enzyme. *Proc Natl Acad Sci USA* 1997; 94: 4262–4266.

37 Chomczynski P, Sacchi N. Single-step method of RNA isolation by acid guanidinium thiocyanate-phenol-chloroform extraction. *Anal Biochem* 1987; 162: 156–159.
38 Maxwell PH *et al*. The interstitial response to renal injury: fibroblast-like cells show phenotypic changes and have reduced potential for erythropoietin gene expression. *Kidney Int* 1997; 52: 715–724.

Original Paper

NEPHRON

Nephron 2002;91:262–269

Accepted: June 13, 2001

Enhanced Expression of C Chemokine Lymphotactin in IgA Nephropathy

Zhou Luo Ou[a] Osamu Hotta[b] Yumiko Natori[a] Hisako Sugai[b]
Yoshio Taguma[b] Yasuhiro Natori[a]

[a]Department of Clinical Pharmacology, Research Institute, International Medical Center of Japan, Tokyo, and
[b]Department of Nephrology, Sendai Shakaihoken Hospital, Sendai, Japan

Key Words
Chemokine · Lymphotactin · IgA nephropathy · Mast cells · MCP-1 · MIP-1β

Abstract
Leukocyte accumulation in the kidney is observed in patients with IgA nephropathy. Chemokines are a large family of cytokines chemotactic for leukocytes and have been shown to be upregulated in renal diseases. We previously reported that the gene expression of lymphotactin, a sole member of C chemokine subfamily, is enhanced in an animal model of crescentic glomerulonephritis, but its expression in human renal diseases is totally unknown. In the present study, we investigated the expression of mRNAs of lymphotactin and some other chemokines in IgA nephropathy. The expression of mRNAs for three chemokines, lymphotactin, MCP-1, and MIP-1β, in renal cortex was increased and the levels of lymphotactin and MCP-1 mRNAs were statistically higher in patients with glomerular crescents than in those without crescents. These levels also correlated with tubulointerstitial changes and urinary protein excretion. Glomerular levels of mRNAs for lymphotactin and MCP-1, but not MIP-1β, were higher in IgA nephropathy than controls. By immunohistochemical analysis, lymphotactin was detected in tryptase-positive cells (putative mast cells) in the interstitial space. These results suggest that lymphotactin, as well as MCP-1, may contribute to leukocyte infiltration and disease progression in IgA nephropathy.

Introduction

IgA nephropathy is the most common form of primary glomerular disease in the world. Chronic renal failure develops in 20–30% of the patients 20 years or more after diagnosis [1]; hence, IgA nephropathy is one of the major causes of end-stage renal disease. As observed in most types of glomerulonephritis, interstitial accumulation of monocytes/macrophages and T lymphocytes is common in IgA nephropathy [2]. Numbers of interstitial mononuclear cells were strongly associated with decreased renal function [3], and these cells are thought to actively participate in interstitial fibrosis and renal dysfunction [4]. Glomerular infiltration of these types of cell in IgA nephropathy is less prominent, but cell number is shown to be significantly increased in IgA nephropathy with active crescents [3, 5], the formation of which is suggested to play an important role in the progression of IgA nephropathy [6].

KARGER
Fax + 41 61 306 12 34
E-Mail karger@karger.ch
www.karger.com

0028–2766/02/0912–0262$18.50/0

Accessible online at:
www.karger.com/journals/nef

Yasuhiro Natori, PhD
Department of Clinical Pharmacology
Research Institute, International Medical Center of Japan
1-21-1 Toyama, Shunjuku-ku, Tokyo 162-8655 (Japan)
Tel. +81 3 3202 7181, Fax +81 3 5273 3038, E-Mail natoriya@ri.imcj.go.jp

In addition, certain clinical features, especially severe proteinuria and persistently elevated serum creatinine, are associated with a poor prognosis [1]. Therefore, mononuclear cells in interstitium and glomeruli are suggested to be invariably involved in the progression of the disease.

Chemokines are a large family of cytokines chemotactic for leukocytes and are considered to play a crucial role in the recruitment and activation of leukocytes in inflammation [7]. They are divided into four groups: CXC, CC, C and CX3C subfamilies, on the basis of the arrangement of the first one or two cysteine residues. Most chemokines fall into CXC or CC groups, whereas only one C and one CX3C chemokine have been identified so far [7]. Because most chemokines specific for monocytes and lymphocytes belong to the CC subfamily, studies on chemokines in renal diseases have mainly focused on CC chemokines [8]. Monocyte chemoattractant protein-1 (MCP-1) is the prototype of CC chemokines and has been shown to react with monocytes, T lymphocytes, natural killer cells, dendritic cells and basophils [7]. An increase of MCP-1 expression is observed in various types of experimental renal diseases [8] and neutralizing antibody to MCP-1 reduced monocyte infiltration in some models [9, 10], suggesting that MCP-1 plays a role, at least in part, in the recruitment of monocytes. The expression of MCP-1 has also been shown in human renal diseases at mRNA and protein levels by histological methods [8], but quantitative analysis on its expression in human kidney has not yet been reported.

Lymphotactin, a sole member of the C chemokine subfamily, has unique characteristics [11]: among nearly twenty chemokine receptors identified, most of which exhibit multiple ligand specificity, the receptor for lymphotactin XCR1 has only one ligand [12]; while other chemokines contain typical four or six cysteine residues, lymphotactin has only two cysteines [13]; lymphotactin has been reported to be chemotactic for T lymphocytes and natural killer cells, but not for monocytes or neutrophils [13, 14]. Although a role for lymphotactin in inflammation has been speculated [11], there have been only few reports showing the induction of lymphotactin in vivo. We previously reported that the gene expression of lymphotactin was enhanced in a rat model of crescentic glomerulonephritis, in parallel with an increase of glomerular CD8-positive cells [15], suggesting that it may also be induced in human glomerulonephritis.

In this study, we attempted to semiquantitatively determine the gene expression of chemokines by reverse transcription-polymerase chain reaction (RT-PCR) and successfully analyzed mRNA levels for three chemokines, lymphotactin, MCP-1 and MIP-1β. We found that mRNA levels for lymphotactin and MCP-1 were enhanced in renal biopsy specimens obtained from patients with IgA nephropathy and that the expression of the two chemokines correlated with clinical and histological parameters associated with progressive IgA nephropathy.

Materials and Methods

Patients and Renal Biopsy Specimens

Biopsy samples were obtained form 39 patients with IgA nephropathy and 5 patients with idiopathic renal hematuria histologically confirmed as isolated C3 deposits disease [16]. Idiopathic renal hematuria used as control in this study was defined as follows: (a) insidious or abrupt onset of gross or microscopic hematuria with little or no proteinuria and no evidence of other features of the nephritic syndrome; (b) minor glomerular abnormalities revealed by light microscopy; (c) blood vessel deposits of C3 without significant glomerular deposition of immunoglobulin or complement revealed by immunofluorescence studies, and (d) absence of any glomerular basement membrane abnormalities by electron microscopy. None of these patients had been treated with steroids or immunosuppressive drugs before biopsy. Serum creatinine level and daily urinary protein excretion were examined at the time of renal biopsy.

All biopsy samples were obtained by surgical needle biopsy and routinely assessed by light microscopic study, immunofluorescence and electron-microscopic study. A part of the specimen was used for immunohistochemical study and RNA analysis. Renal biopsies of patients with IgA nephropathy were examined histologically and graded (by O.H.) without knowledge of the results of chemokine analysis. Two histological parameters were evaluated on the basis of their established prognostic value. First, biopsies were divided into those with (n = 16) and without (n = 23) crescent formation under microscopic examination. Second, tubulointerstitial changes were assessed by measuring the affected areas of interstitial mononuclear cell infiltration, tubular atrophy and interstitial fibrosis by the method of Hewitson and Becker [17]. The affected area was quantitated by point counting using an eyepiece graticule of 1 cm^2 with ten equidistant lines at a final magnification of × 400.

Glomeruli were collected from a piece of the biopsy specimens under a dissecting microscope. Five or more glomeruli could be isolated from 28 of 39 specimens of patients with IgA nephropathy and from 5 of 5 of control patients. These isolated glomeruli (IgA nephropathy, n = 28; control, n = 5) as well as samples of whole renal cortex (IgA nephropathy, n = 39; control, n = 5) were separately used for the preparation of total RNA.

RNA Analysis

Total RNA was extracted from renal cortex and isolated glomeruli with ISOGEN kit (Wako Pure Industries, Osaka, Japan). RNA content in the fraction from renal cortex was measured by RiboGreen RNA quantitation kit (Molecular Probes, Eugene, Oreg., USA). Because RNA content in glomerular RNA preparations was too small to be measured, the content in each sample was estimated based on the number of glomeruli used of RNA isolation. Normal splenic tissue was obtained from a patient undergoing tumor splenectomy and its total RNA was prepared and used as a positive control.

Table 1. PCR primers and size of PCR products

	5′primers	3′ primers	Size, bp
Lymphotactin	GACTTCTCATCCTGGCCCTCCTTG	GTATTGGTCGATTGCTGGGTTCCTG	319
MCP-1	ACTGAAGCTCGCACTCTCGCCTC	TGTCTGGGGAAAGCTAGGGGAAAAT	389
MIP-1β	TGTCCTGTCTCTCCTCATGCTAGTA	GCTCAGTTCAGTTCCAGGTCATACA	264
GAPDH	GGGAGCCAAAAGGGTCATCATCTC	CCATGCCAGTGAGCTTCCCGTTC	516

As a template of RT-PCR, 0.1 ng (GAPDH), 0.1 μg (MCP-1, lymphotactin) or 0.2 μg (MIP-1β) of renal cortex RNA or RNA isolated from a half (MIP-1β, GAPDH) or one (MCP-1, lymphotactin) glomerulus was used. Reverse transcription was carried out at 42°C for 50 min in 10 μl of buffer containing 20 m*M* Tris-HCl, pH 8.4, 50 m*M* KCl, 2.5 m*M* $MgCl_2$, 100 μg/ml bovine serum albumin, 1 m*M* each of dATP, dCTP, dGTP and dTTP, 0.25 μg oligo(dT) $_{12-18}$ and 100 U M-MLV Reverse Transcriptase (Gibco BRL, Gaithersburg, Md., USA). Reactions were stopped by heat inactivation at 90°C for 5 min and chilled on ice. Subsequently, the cDNA was amplified in 25 μl of 10 m*M* Tris-HCl (pH 9.0) containing 50 m*M* KCl, 1.5 m*M* $MgCl_2$, 0.2 m*M* 5′ and 3′ primers (table 1), and 1.25 U AmpliTaq Gold DNA polymerase (Perkin Elmer, Foster, Calif., USA). The amplification reaction was carried out for a total of 45 cycles as follows: denaturation for 30 s at 95°C, annealing for 30 s at 54°C (lymphotactin), 60°C (MCP-1, GAPDH), or 64°C (MIP-1β), and extension for 1 min at 72°C. For semiquantitative analysis, the amount of RNA for reverse transcription and the PCR cycle numbers were chosen in order to avoid excessive amplification. According to the manufacturer's instruction, PCR using AmpliTaq Gold DNA polymerase requires 5–10 cycles more than common DNA polymerases because of its characteristics. The products of PCR were separated by electrophoresis on a 2% agarose gel with ethidium bromide staining. The intensity of bands of cDNAs was quantified by computer-analyzed densitometry and the values for chemokine mRNAs were normalized to those for GAPDH mRNA. Data were analyzed by Mann-Whitney U test or Spearman rank correlation and a value of $p < 0.05$ was considered statistically significant.

Immunohistochemical Analysis

The biotin-streptavidin-peroxidase method with a Histofine kit (Nichirei, Tokyo, Japan) was used for immunohistochemical analysis as described previously [18]. Briefly, 3-μm thick sections of formalin-fixed paraffin-embedded tissue were deparaffinized in xylene, and endogenous peroxidase activity was blocked by incubating for 10 min in 3% hydrogen peroxide. After incubation with 10% fetal calf serum in phosphate-buffered saline, the sections were allowed to react with dilutions of the primary antibodies for 40 min, followed by the incubation for 30 min with a second biotinylated antibody.

The primary antibodies used in the present study were: rabbit polyclonal antihuman lymphotactin antibody (PetroTech EC Ltd., London, UK), mouse monoclonal antibodies to human mast cell tryptase (AA1, DAKO, Copenhagen, Denmark), CD68 (PG-M1, DAKO) for the detection of macrophages, and CD45RO (UCHL-1, DAKO) for the detection of memory T lymphocytes. A mirror section analysis [19] was performed for the identification of lymphotactin-producing cells. Two serial sections were obtained with the cut surfaces facing each other, and each section was reacted either with antihuman lymphotactin antibody or with antibodies to tryptase, CD68, or CD45RO.

Results

Chemokine mRNA Levels in Renal Cortex

RNA content extracted from 39 renal cortex preparations was determined in the range between 1.4 and 3.2 μg and we considered that the content was not enough to be used for quantitative RT-PCR methods which we previously reported [20]. Then we attempted to detect mRNAs for totally 11 chemokines and cytokines (MCP-1, MCP-3, MIP-1α, MIP-1β, RANTES, I-309, lymphotactin, IL-8, IP-10, IL-1β, TNF-α) in several biopsy specimens with 0.2 μg of RNA fraction at most and found that mRNAs for three chemokines, MCP-1, MIP-1β and lymphotactin, could be semiquantitatively determined by RT-PCR: The amplification performed with differential PCR cycles up to 45 or with serially lower amounts of RNA confirmed a cycle- and dose-dependent increase of the PCR products (data not shown). Because levels of mRNAs for the other chemokines and cytokines were not semiquantitatively determined, levels of the three chemokine mRNAs of all samples were subsequently analyzed.

Figure 1 shows the electrophoretogram of the products of RT-PCR for lymphotactin, MCP-1, and MIP-1β using RNA isolated from renal cortex. There was very low or no levels of the expression of the chemokine mRNAs in controls, whereas marked expression was observed in the group of patients with IgA nephropathy. Figure 2 shows the results of the densitometric analysis of the products of RT-PCR. The upregulation of the three chemokines in patients with IgA nephropathy was statistically significant and that of lymphotactin and MCP-1 mRNA was more prominent.

Out of 39 patients with IgA nephropathy, 23 were crescent negative and 16 were crescent positive under light-

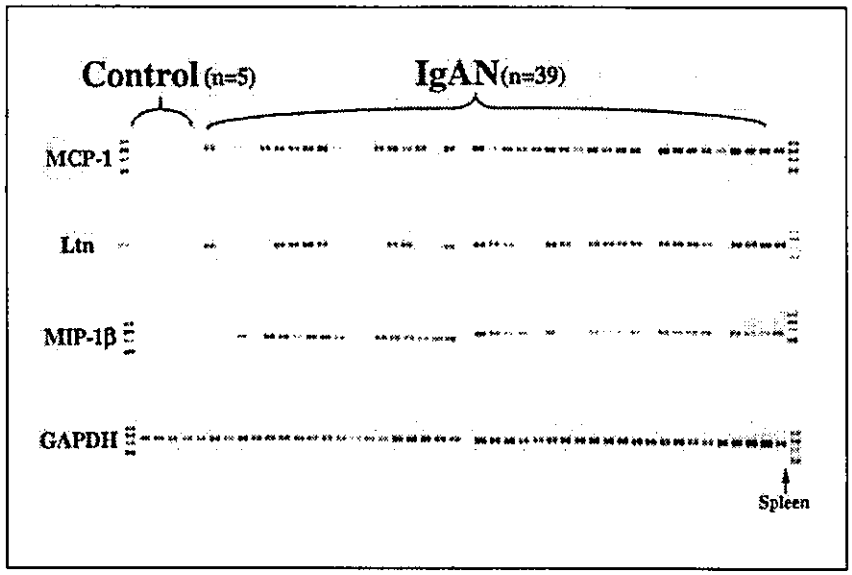

Fig. 1. RT-PCR products of mRNAs for chemokines and GAPDH using RNA prepared from renal cortex of 39 patients with IgA nephropathy and 5 control patients. The black/white contrast has been reversed.

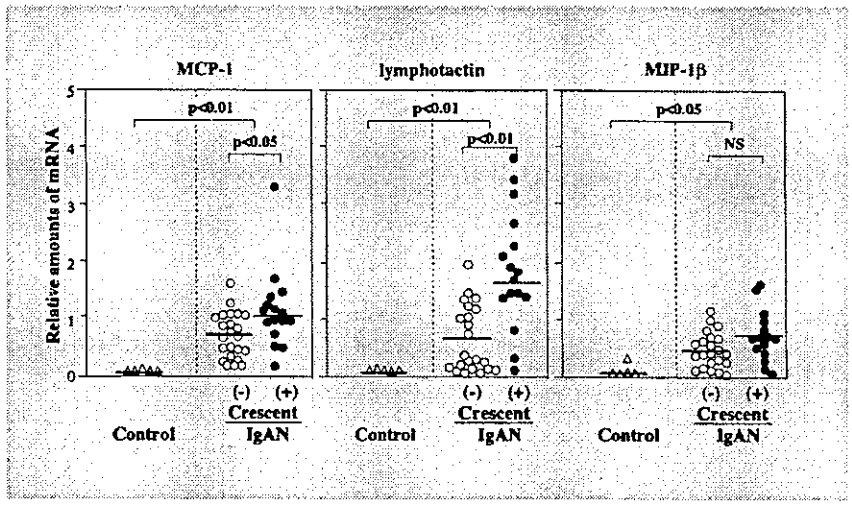

Fig. 2. Expression of chemokine mRNAs in renal cortex of patients with IgA nephropathy. △ = Control; ○ = IgA nephropathy without glomerular crescents; ● = IgA nephropathy with glomerular crescents. Each symbol represents an individual patient with bars depicting means for each group.

microscopic examination. As shown in figure 2, the levels of lymphotactin and MCP-1 mRNAs in patients with crescents were significantly higher than those without crescents, although there was considerable overlap, especially of MCP-1. There was no difference in the level of MIP-1β between the two groups. The levels of lymphotactin and MCP-1 mRNAs also correlated with tubulointerstitial changes and urinary protein excretion (fig. 3), but that of MIP-1β mRNA did not (data not shown). Thus, the levels of the gene expression of lymphotactin and MCP-1, but not MIP-1β, correlated with the clinical and histological severity of IgA nephropathy. The levels of the chemokine mRNAs did not correlate with serum creatinine level (data not shown).

Chemokine mRNA Levels in Glomeruli

Levels of mRNAs for the three chemokines in glomerular RNA samples were measured by the same method as those in renal cortex, except for the amount of RNA. Glomerular expression of lymphotactin and MCP-1 mRNAs, but not MIP-1β mRNA was significantly enhanced in patients with IgA nephropathy (fig. 4, 5). In contrast to renal cortex, there was no significant difference in the levels of mRNAs for lymphotactin and MCP-1 between cres-

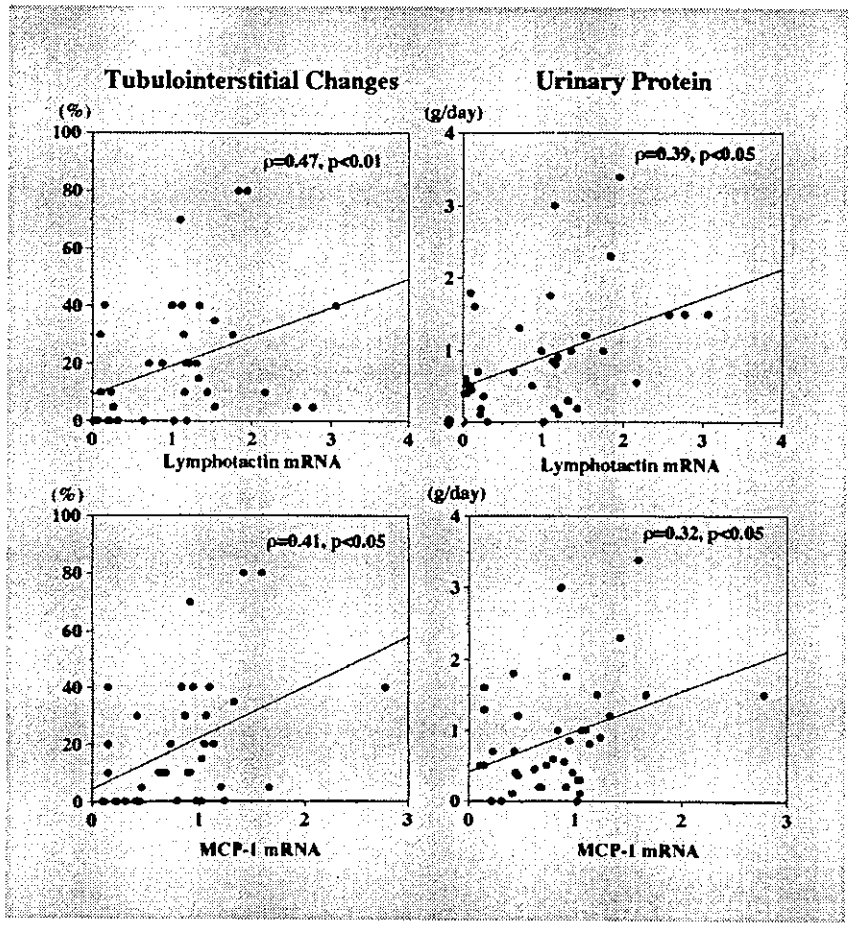

Fig. 3. Correlation of lymphotactin and MCP-1 mRNAs in renal cortex with tubulointerstitial changes and urinary protein excretion. Each dot represents and individual patient.

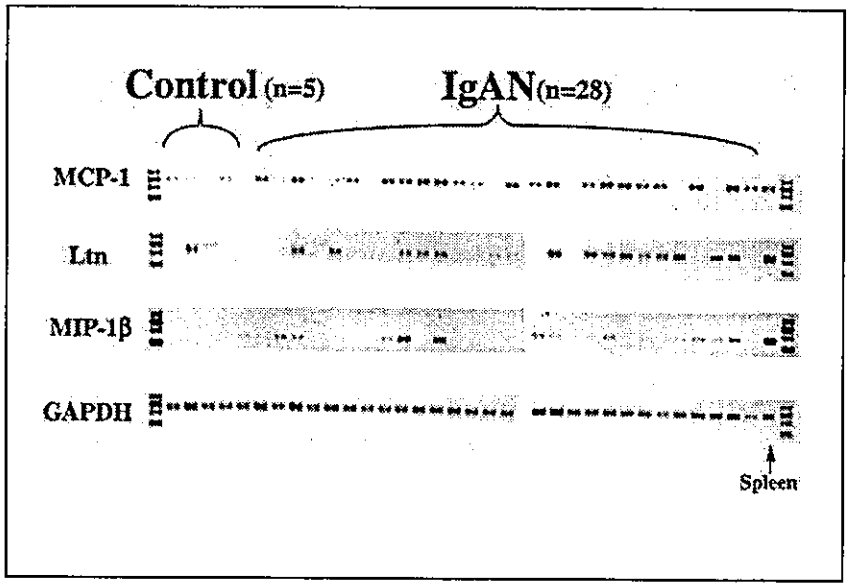

Fig. 4. RT-PCR products of mRNAs for chemokines and GAPDH using glomerular RNA of 28 patients with IgA nephropathy and 5 control patients. The black/white contrast has been reversed.

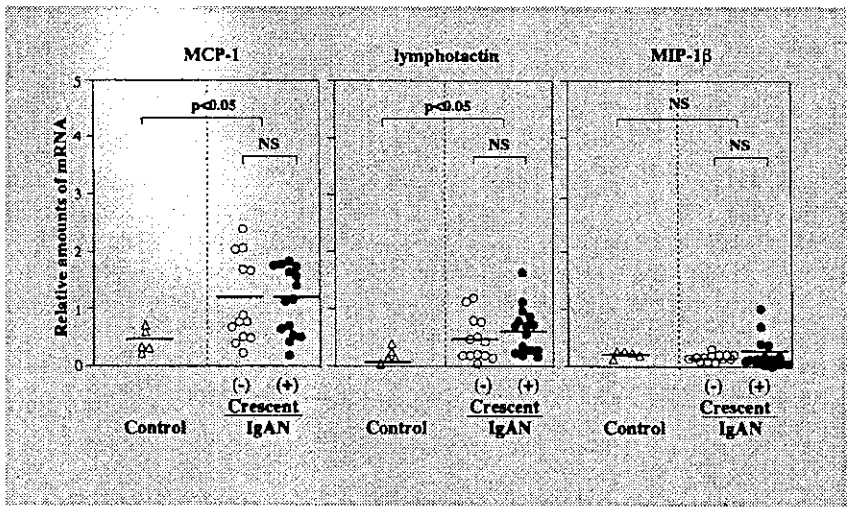

Fig. 5. Glomerular expression of chemokine mRNAs in patients with IgA nephropathy. △ = Control; ○ = IgA nephropathy without glomerular crescents; ● = IgA nephropathy with glomerular crescents. Each symbol represents an individual patient with bars depicting means for each group.

cent-positive and crescent-negative patients (fig. 5). The levels did not correlate with the level of urinary protein, tubulointerstitial changes, or serum creatinine (data not shown). Although there was no difference in the level of MIP-1β mRNA between patients with IgA nephropathy and control, the level of MIP-1β mRNA in IgA nephropathy patients correlated with their serum creatinine level ($\rho = 0.496$, $p < 0.05$).

Immunohistochemistry

The production of lymphotactin at the protein level and its localization in the kidney in IgA nephropathy were tested. Lymphotactin-positive cells were detected in the interstitium (fig. 6, left), but were virtually absent in glomeruli (data not shown). In contrast, lymphotactin-positive cells were negligible both in the interstitium and glomeruli in control kidneys (data not shown). We used the mirror section method to elucidate the phenotype of the lymphotactin-positive cells. The expression of lymphotactin were restricted to tryptase-positive cells, but not to CD68-positive (macrophages) or CD45RO-positive (memory T lymphocytes) cells (data not shown).

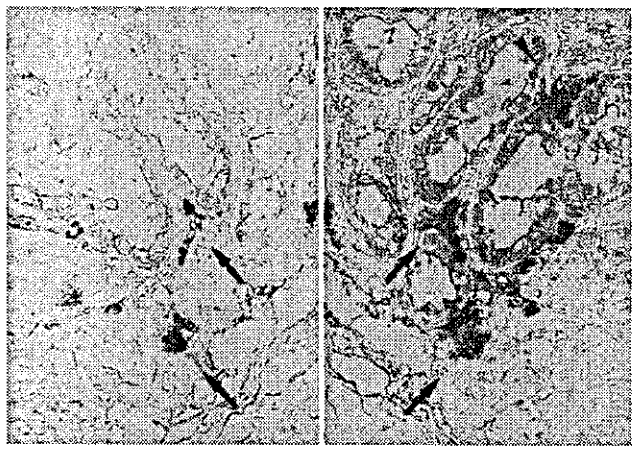

Fig. 6. Localization of lymphotactin in the kidney of a patient with IgA nephropathy. Mirror sections were stained with antibodies to lymphotactin (left) or tryptase (right). Note that there are cells positive for both lymphotactin and tryptase (arrows) and those only positive for tryptase (arrowhead).

Discussion

The present study demonstrates that the expression of lymphotactin is enhanced in the kidney of patients with IgA nephropathy. In addition, the level of lymphotactin mRNA in renal cortex correlated with glomerular crescent formation, tubulointerstitial changes and the level of urinary protein, which are three factors associated with a poor prognosis in IgA nephropathy. These results suggest that lymphotactin may be involved in the mechanisms of the progression of IgA nephropathy. The present study also shows that the transcriptional level of MCP-1 in the kidney is upregulated in IgA nephropathy and correlates with the clinical and histological parameters, in agreement with the previous studies that suggest the contribution of MCP-1 to the progression of renal diseases [8].

In contrast to MCP-1, the information about lymphotactin in inflammatory diseases including glomerulonephritis is extremely limited. We have previously reported that the transcription of lymphotactin is upregulated in an experimental model of crescentic glomerulonephritis, corresponding with the increase of glomerular CD8-positive cells [15], the cell type essential for the initiation of the disease model [21]. On the other hand, in a model of transient proteinuria [22], in which mild interstitial infiltration of monocytes but not lymphocytes is observed, the enhanced transcription of MCP-1, but not lymphotactin was detected [20]. Therefore, it is plausible that the upregulation of lymphotactin might be more limited than that of MCP-1 in renal diseases.

The transcriptional levels of the two chemokines correlated with the level of urinary protein, but not with the level of serum creatinine. Because proteinuria per se is suggested to cause tubulointerstitial injury as well as inflammation [23], our results may imply that chemokine production in tubulointerstitium is more closely related to the level of urinary protein than to that of serum creatinine. Glomerular levels of mRNA for these two chemokines did not show any correlation with clinical or histological parameters including glomerular crescents. Because glomerular changes might be focal, it is conceivable that variation of the chemokine expression among each glomerulus may cause such observation.

Our immunohistological studies confirmed the gene expression of lymphotactin at the protein level. Lymphotactin was detected in some of the interstitial cells which were positive for tryptase staining, a marker of mast cells [24]. In culture, lymphotactin mRNA is expressed by activated CD8-positive T lymphocytes [13] and also by other hematopoietic cells [25]. Rumsaeng et al. [26] reported that human and murine mast cell lines and murine bone marrow-cultured mast cells produce lymphotactin following Fcε receptor I aggregation. The present study demonstrates that tryptase-positive cells, possibly mast cells produce lymphotactin in humans in vivo. We could not detect glomerular expression of lymphotactin protein, probably due to less sensitivity of immunohistochemistry for secreted proteins such as chemokines, compared with RT-PCR analysis.

Recent studies have suggested that, in addition to being a major effector cell in the elicitation of allergic inflammation, mast cells are activated in various T lymphocyte-mediated inflammatory processes [27]. Previously the increase of interstitial mast cells in IgA nephropathy and other renal diseases was reported [28–30] and there was a strong correlation between the number of mast cells and the number of interstitial T lymphocytes in rapidly progressive glomerulonephritis [30]. Because the T lymphocyte is one of the target cell types of lymphotactin, it is speculated that lymphotactin and other cytokines and chemokines produced by mast cells may contribute to the recruitment of T lymphocytes and the progression of glomerulonephritis.

Acknowledgments

We thank Dr. David J. Salant, Boston Medical Center, for his critical review of the manuscript. We also thank Mr. H. Kitamura, Sendai Shakaihoken Hospital, for his histological assistance. This work was supported in part by Health Science Research Grant (Research on Specific Diseases) from Ministry of Health and Welfare.

References

1 Glassock RJ, Cohen AH, Adler SG: Primary glomerular diseases; in Brenner BM (ed): The Kidney, ed 5. Philadelphia, Saunders, 1996, pp 1392–1497.
2 Hooke DH, Gee DC, Atkins RC: Leukocyte analysis using monoclonal antibodies in human glomerulonephritis. Kidney Int 1987,31: 964–972.
3 Li H-L, Hancock WW, Hooke DH, Dowling JP, Atkins RC: Mononuclear cell activation and decreased renal function in IgA nephropathy with crescents. Kidney Int 1990;37:1552–1556.
4 Schena FP, Gesualdo L, Grandaliano G, Montinaro V: Progression of renal damage in human glomerulonephritides: Is there sleight of hand in winning the game? Kidney Int 1997; 52:1439–1457.
5 Hotta O, Taguma Y, Ooyama M, Yusa N, Nagura H: Analysis of CD14+ cells and CD56+ cells in urine using flow cytometry: A useful tool for monitoring disease activity of IgA nephropathy. Clin Nephrol 1993;39:289–294.
6 Abe T, Kida H, Yoshimura M, Yokoyama H, Koshino Y, Tomosugi N, Hattori N: Participation of extracapillary lesions (ECL) in progression of IgA nephropathy. Clin Nephrol 1986; 25:37–41.
7 Luster AD: Chemokines, chemotactic cytokines that mediate inflammation. N Engl J Med 1998;338:436–445.
8 Rovin BH, Phan LT: Chemotactic factors and renal inflammation. AM J Kidney Dis 1998; 31:1065–1084.
9 Tang WW, Qi MY, Warren JS: Monocyte chemoattractant protein 1 mediates glomerular macrophage infiltration in anti-GBM Ab GN. Kidney Int 1996;50:665–671.
10 Wada T, Yokoyama H, Furuichi K, Kobayashi KI, Harada K, Naruto M, Su SB, Akiyama M, Mukaida N, Matsushima K: Intervention of crescentic glomerulonephritis by antibodies to monocyte chemotactic and activating factor (MCAF/MCP-1). FASEB J 1996;10:1418–1425.
11 Hedrick JA, Zlotnik A: Lymphotactin. Clin Immunol Immunopathol 1998;87:218–222.
12 Yoshida T, Imai T, Kakizaki M, Nishimura M, Takagi S, Yoshie O: Identification of single C motif-1/lymphotactin receptor XCR1. J Biol Chem 1998;273:16551–16554.

13 Kelner GS, Kennedy J, Bacon KB, Kleyensteuber S, Largaespada DA, Jenkins NA, Copeland NG, Bazan JF, Moore KW, Schall TJ, Zlotnik A: Lymphotactin: A cytokine that represents a new class of chemokine. Science 1994;266: 1395–1399.
14 Giancarlo B, Silvano S, Albert Z, Mantovani A, Allavena P: Migratory response of human natural killer cells to lymphotactin. Eur J Immunol 1996;26:3238–3241.
15 Natori Yu, Ou ZL, Yamamoto-Shuda Y, Natori Y: Expression of lymphotactin mRNA in experimental crescentic glomerulonephritis. Clin Exp Immunol 1998;113:265–268.
16 Grekas D, Morley AR, Wilkinson R, Kerr NS: Isolated C3 deposition in patients without systemic disease. Clin Nephrol 1984;21:270–274.
17 Hewitson TD, Becker GJ: Interstitial myofibroblasts in IgA glomerulonephritis. Am J Nephrol 1995;15:111–117.
18 Oda T, Hotta O, Taguma Y, Kitamura H, Sudo K, Horigome I, Chiba S, Yoshizawa N, Nagura H: Involvement of neutrophil elastase in crescentic glomerulonephritis. Hum Pathol 1997; 28:720–728.
19 Fukushima K, Masuda T, Ohtani H, Sasaki I, Funayama Y, Masuno S, Nagura H: Immunohistochemical characterization, distribution and ultrastructure of lymphocytes bearing the gamma/delta T-cell receptor in the human gut. Virchows Arch [B] 1991;60:7–13.
20 Ou ZL, Natori Yu, Doi N, Kawasaki K, Nishijima M, Natori Y: Competitive reverse transcription-polymerase chain reaction for determination of rat CC and C chemokine mRNAs. Anal Biochem 1998;261:227–229.
21 Kawasaki K, Yaoita E, Yamamoto T, Kihara I: Depletion of CD8 positive cells in nephrotoxic serum nephritis of WKY rats. Kidney Int 1992; 41:1517–1526.
22 Salant DJ, Natori Y, Shimizu F: Glomerular injury due to antibody alone; in Neilson EG, Couser WG (eds): Immunologic Renal Diseases. New York, Raven Press, 1997, pp 359–375.
23 Chen L, Wang Y, Tay Y-C, Harris DCH: Proteinuria and tubulointerstitial injury. Kidney Int 1997;52:S60–S62.
24 Irani AA, Schechter NM, Craig SS, DeBlois G, Schwartz LB: Two types of human mast cells that have distinct neutral protease compositions. Proc Natl Acad Sci USA 1986;83:4464–4468.
25 Hedrick JA, Saylor V, Figueroa D, Mizoue L, Xu YM, Menon S, Abrams J, Handel T, Zlotnik A: Lymphotactin is produced by NK cells and attracts both NK cells and T cells in vivo. J Immunol 1997;158:1533–1540.
26 Rumsaeng V, Vliagoftis H, Oh CK, Metcalfe DD: Lymphotactin gene expression in mast cells following Fc epsilon receptor I aggregation: Modulation by TGF-beta, IL-4, dexamethasone, and cyclosporin A. J Immunol 1997;158:1353–1360.
27 Mekori YA, Metcalfe DD: Mast cell-T cell interactions. J Allergy Clin Immunol 1999;104: 517–523.
28 Ehara T, Shigematsu H: Contribution of mast cells to the tubulointerstitial lesions in IgA nephritis. Kidney Int 1998;54:1675–1683.
29 Hiromura K, Kurosawa M, Yano S, Naruse T: Tubulointerstitial mast cell infiltration in glomerulonephritis. Am J Kidney Dis 1998;32: 593–599.
30 Toth T, Toth-Jakatics R, Jnimi S, Ihara M, Urata H, Takebayashi S: Mast cells in rapidly progressive glomerulonephritis. J Am Soc Nephrol 1999;10:1498–1505.

NEPHRON

Original Paper

Nephron 2002;91:710–718

Accepted: August 28, 2001

Prepubertal Treatment with Angiotensin Receptor Blocker Causes Partial Attenuation of Hypertension and Renal Damage in Adult Dahl Salt-Sensitive Rats

Hideaki Nakaya Hiroyuki Sasamura Mizuo Mifune Ryoko Shimizu-Hirota
Mari Kuroda Matsuhiko Hayashi Takao Saruta

Department of Internal Medicine, School of Medicine, Keio University, Tokyo, Japan

Key Words

Dahl salt-sensitive rat · Nephrosclerosis · Angiotensin receptor blocker

Abstract

Recently, we have shown that treatment of stroke-prone spontaneously hypertensive rats with angiotensin inhibitors for a limited time-window before puberty results in an attenuation of hypertensive nephrosclerosis in later life. The aim of this study was to examine the applicability of this therapeutic paradigm to a low-renin model. Dahl salt-sensitive (Dahl-S) rats were fed a high-salt diet from age 6 weeks. Some rats were treated with the angiotensin receptor blocker (ARB) candesartan cilexetil (2 mg/kg/d) from weaning to puberty (age 3–10 weeks), whereas other rats were treated continuously until overt renal damage was seen (age 3–16 weeks). Dahl-S rats on a high salt diet had increased blood pressure (207 ± 3 vs. 125 ± 2 mm Hg), proteinuria, and glomerular/vascular histological changes. The prepubertal treatment with ARB resulted in a continued suppression of blood pressure (153 ± 2 mm Hg) at 16 weeks. Both proteinuria and renal histological changes were significantly ($p < 0.05$) attenuated, but not completely prevented by the treatment. No significant differences in plasma renin activity, renin mRNA, or AT1/AT2 mRNA were seen between groups. These results suggest that prepubertal treatment affords sustained renoprotection, even in an animal model with a suppressed renin-angiotensin system, and support the notion that appropriate prepubertal intervention may lead to a partial attenuation in the susceptibility to inherited renal diseases.

Introduction

Hypertension is a leading cause of morbidity and mortality, and hypertensive complications such as ischemic heart disease, heart failure, and renal failure pose an ever greater burden on medical resources. It has been estimated that up to 20% of the general population is hypertensive, and of these nearly half may have a form of hypertension which is exacerbated by a high salt diet ('salt-sensitive hypertension') [1].

Until recently, the emphasis in the treatment of hypertension has been on life-long treatment with antihypertensive agents. The development of newer classes of antihypertensive agents with increased tolerability, a favourable side-effect profile, and greater protection against end-organ damage has made treatment of hypertension theoretically much easier than before.

KARGER

Fax + 41 61 306 12 34
E-Mail karger@karger.ch
www.karger.com

0028–2766/02/0914–0710$18.50/0

Accessible online at:
www.karger.com/journals/nef

Hiroyuki Sasamura, MD, PhD
Department of Internal Medicine, School of Medicine
Keio University, 35 Shinanomachi, Shinjuku-ku
Tokyo 160-8582 (Japan)
Tel. +81 3 3353 1211, Fax +81 3 3359 2745, E-Mail sasamura@med.keio.ac.jp

Despite the widespread use of these newer classes of agents, optimal treatment of hypertension remains elusive. Consequently, hypertensive nephrosclerosis remains a leading cause of end-stage renal failure requiring dialysis, and the incidence of this disease continues to rise in many countries. One of the key reasons may be that the current forms of antihypertensive treatment are palliative, and do not offer a complete cure for hypertension.

Previous studies have shown that treatment of spontaneously hypertensive rats (SHR) with angiotensin-converting enzyme inhibitors (ACEI) or angiotensin receptor blockers (ARB) for a limited period during development is effective in permanently attenuating the development of hypertension [2–5]. Similar findings have been reported by Katovich et al., using a retrovirus containing antisense to ACE or the angiotensin receptor [6]. Recently, we have shown that this prepubertal treatment also results in a sustained protection from renal injury in stroke-prone SHR (SHRSP), and that the mechanism for these effects may be related to suppression of the renin-angiotensin system, since overactivation of the renin-angiotensin system has been shown to be one of the important mechanisms related to the onset of renal injury in these rats [5].

To date, all of these studies have been performed using one animal model with an activated renin-angiotensin system (the SHR) so it is unclear at present whether these findings are specific to the SHR model of hypertension, or are generally applicable to all forms of hypertension. It is particularly important to clarify this question, because if the effect is general and not specific to the SHR, then it increases the hope that appropriate intervention may result in a 'cure' of hypertension, irrespective of the genetic cause. Therefore in this study, we examined for the first time the effects of prepubertal ARB treatment in a different model of genetic hypertension and renal damage. Specifically, we tested the hypothesis that early treatment with ARB may provide long-lasting protection against hypertension and/or renal damage, even in an animal model with a markedly suppressed renin-angiotensin system.

Methods

Animal Treatments

Studies were conducted using 3-week-old male Dahl-S rats maintained by Sankyo Laboratories, Tokyo, Japan. All experiments were performed in accordance with the Animal Experimentation Guidelines of Keio University School of Medicine. All rats were initially fed a normal salt diet (CE-2, Nippon Clea, Japan) containing 0.3% NaCl. At age 6 weeks, most of the rats were changed to a high salt diet (8% NaCl). Drinking water was monitored daily using drinking bottles. Rats were housed 6 to a cage except for the period of urine collection for protein measurements, when they were housed individually in metabolic cages. Rats were randomly divided into 4 groups (n = 6 per group). Rats in group 1 were control Dahl-S rats which were kept on a normal salt diet throughout the experiment. Rats in group 2–4 were kept on a normal salt diet from age 3–6 weeks, then changed to a high salt diet until the end of the experiment. In addition, the rats in groups 3 and 4 were treated from age 3–10 weeks (group 3), or from age 3–16 weeks (group 4) with the ARB candesartan cilexetil (dissolved in drinking water (0.01 g/l) as described by Mackenzie et al. [7]); the calculated dose for a 250 g rat drinking 50 ml/day is 2 mg/kg/day). At 16 weeks, one rat from each of the groups 1, 2, and 4 died, at which point the experiment was terminated. Although confirmatory autopsies were not performed, the symptoms in these rats were suggestive of stroke.

Assays

Systolic blood pressure and heart rate of awake animals were measured by tail-cuff plethysmography using a Natsume KN-210 manometer. 24 h urine collections were performed in metabolic cages (every 2 weeks from age 5–13 weeks, then weekly thereafter), and urinary protein concentrations were determined using an autoanalyzer. Rats were sacrificed by decapitation, and trunk blood was collected in pre-chilled beakers containing the inhibitors 0.1 m*M* phenylmethylsulfonylfluoride (PMSF), 3.5 m*M* ethylenediaminetetraacetate (EDTA), and 0.12 m*M* pepstatin. Samples were immediately centrifuged at 4 °C, and stored at –20 °C. Plasma renin activity was determined by radioimmunoassay of angiotensin I formed by incubation of plasma for 1 h at 37 °C. Plasma angiotensin II levels were analyzed by radioimmunoassay as described previously [5, 8]. Other blood chemistries were measured using an autoanalyzer.

Histological Studies

Kidneys and thoracic aortae were fixed in 10% phosphate-buffered formalin, then embedded in paraffin blocks. Histologic sections from the rat kidneys were stained with PAS, and sections from aortae were stained with Azan. Slides were examined by light microscopy, and renal histopathological changes were scored as described previously [5, 8]. For the assessment of glomerular damage, over 50 glomeruli were examined and the number of glomeruli exhibiting focal or global ischemic or proliferative damage was enumerated and expressed as a percentage of the total number of glomeruli examined. Blood vessels were graded 0–4 for arteriolar sclerosis according to the severity of hyalinosis and thickening of the vascular wall in small-medium sized arteries. Tubulointerstitial changes, including interstitial inflammation and tubular atrophy, were assessed and graded 0–3: grade 1 was involvement of <20% of the cortical interstitium, grade 2 was involvement of 20–40% of the interstitium and grade 3 was involvement >40%.

RT-PCR (Reverse Transcription-Polymerase Chain) Analysis of Renal Gene Expressions

Total RNA was purified from rat kidneys by the acid guanidine-phenol-chloroform method, and quantified by measurement of absorbance at 260 nm in a spectrophotometer. Renin, AT1 and AT2 receptor subtype mRNA were analyzed by semi-quantitative RT-PCR, as reported by us previously [5, 8]. In brief, 1 μg total RNA was reverse transcribed in a reaction mixture containing 10 m*M* Tris HCl (pH 8.3), 50 m*M* KCl, 5 m*M* $MgCl_2$, 1 m*M* dNTP, 1 U RNase inhib-

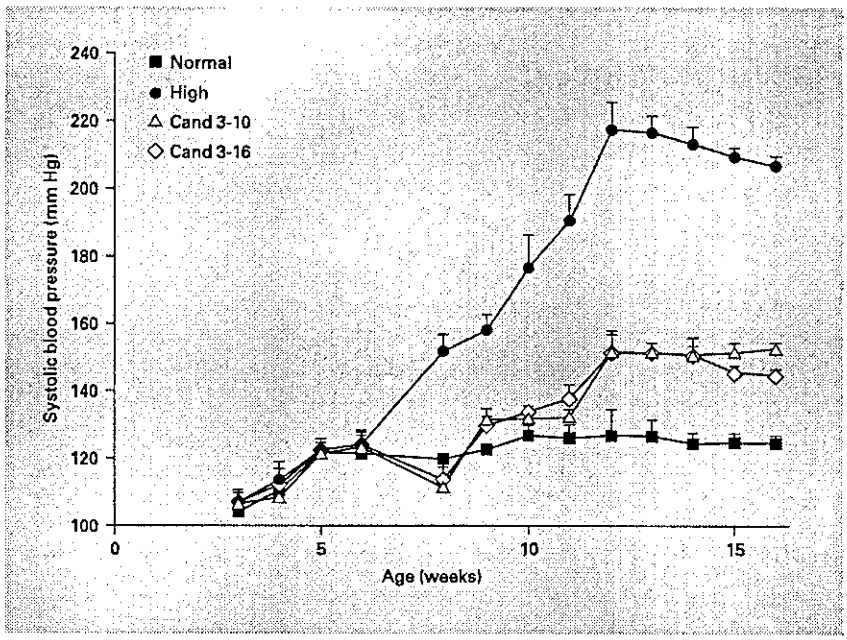

Fig. 1. Effects of treatment of pre-pubescent rats with candesartan cilexetil (2 mg/kg/d) on blood pressure in Dahl-S rats. Normal: group 1 (normal salt diet); High: group 2 (high salt diet); Cand 3–10: group 3 (high salt diet + candesartan cilexetil (3–10 weeks)); Cand 3–16: group 4 (high salt diet + candesartan cilexetil (3–16 weeks)). Blood pressures in the Cand 3–10 and Cand 3–16 groups were significantly reduced compared to the High group at all time points after week 7. A significant difference was also seen between Cand 3–10 and Cand 3–16 at weeks 15 and 16 ($p < 0.01$, symbols omitted for clarity).

itor, 2.5 μ*M* (50 pmol) random hexamers and 2.5 U Moloney murine leukemia virus reverse transcriptase in a volume of 20 μl. The reverse transcribed product was amplified with renin, AT1, AT2 or GAPDH sense and antisense primers in a reaction mixture containing 10 m*M* Tris HCl (pH 8.3), 50 m*M* KCl, 2 m*M* $MgCl_2$, 0.2 m*M* dNTP, 15 pmol of each primer, 5 μCi ^{32}P-dCTP, and 2.5 U Taq polymerase using a Perkin-Elmer-Cetus thermal cycler for 24 cycles. Renin primers were 5′-TGCCACCTTGTTGTGTGAGG-3′ and 5′-ACCCGATGCGATTGTTATGCCG-3′ which correspond to sense and antisense respectively, of bases 851–870 bp and 1203–1224 bp in the rat renin sequence. AT1 primers were 5′-GGAAACAGCTTGGTGGTG-3′ and 5′-GCACAATCGCCATAATTATCC-3′ corresponding to bases 133–150 and antisense of 719–739 in the rat AT1a and AT1b sequences. AT2 primers were 5′-ATGAAGGACAACTTCAGTTTTGC-3′ and 5′-CAAGGGGAACTACATAAGATG-3′ (bases 1–23 and antisense of 478–499 respectively). GAPDH primers were 5′-TCCCTCAAGATTGTCAGCAA-3′ and 5′-AGATCCACAACGGATACATT-3′ (bases 451–470 and antisense of 739–758 respectively). To assess relative levels of AT1a and AT1b amplified PCR product, the PCR product was incubated for 90 min at 37 °C in the presence of EcoRI (10 units). Because the AT1a (but not AT1b) receptor contains an internal EcoRI site, EcoRI digestion under these conditions results in two fragments of length 428 bp and 178 bp in the case of AT1a DNA, and one fragment of length 606 bp in the case of AT1b. Preliminary experiments confirmed that these PCR reactions were performed within the linear phase of the PCR amplification reaction. Reaction products were resolved by electrophoresis through 8% polyacrylamide gels. Gels were dried using a gel dryer and incorporated radioactivity in each band was quantified with a laser image analyzer (model BAS 2000; Fuji Film Co., Tokyo Japan).

Materials

Candesartan cilexetil were generously provided by Takeda Chemical Industries Ltd. RT-PCR and electrophoresis reagents were obtained from Perkin Elmer and Biorad. Other chemicals were from Sigma.

Statistics

Results are expressed as the mean ± SEM. Statistical comparisons were made by ANOVA followed by Fisher's Protected Least Significant Difference (PLSD) test for comparison between groups. Values of $p < 0.05$ were considered statistically significant.

Results

Effects of Treatment of Pre-Pubescent Rats with Candesartan Cilexetil on Blood Pressure in Dahl-S Rats

As shown in figure 1, all the rats had a blood pressure of approximately 120 mm Hg at 6 weeks. In the case of the rats in group 1, which were maintained on the normal salt diet, blood pressure remained at this value for the duration of the experiment. In contrast, the blood pressure of the rats in group 2, which were changed to a high salt diet at 6 weeks, rose to a value of 200–220 mm Hg after the diet change. The elevation in blood pressure was attenuated (to approximately 150 mm Hg) in the rats in group 4 treated with candesartan cilexetil from 3–16 weeks. Of

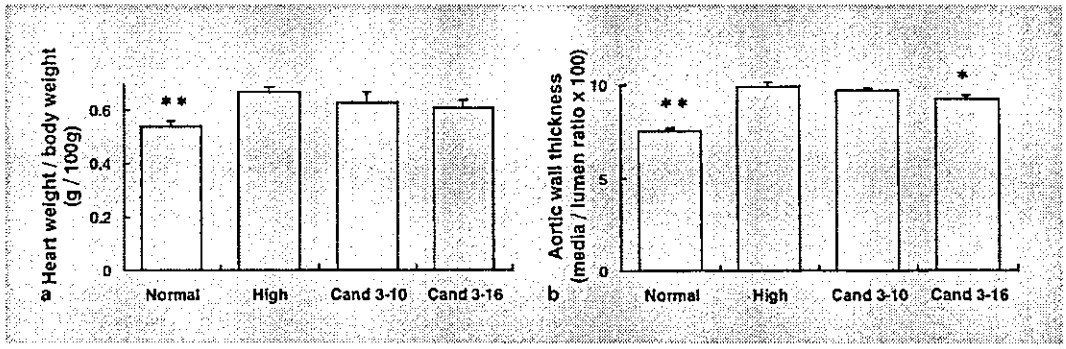

Fig. 2. Effects of treatment of pre-pubescent rats with candesartan cilexetil (2 mg/kg/d) on (**a**) heart weight/body weight ratios and (**b**) aortic wall thickness at 16 weeks in Dahl-S rats. Normal: group 1 (normal salt diet); High: group 2 (high salt diet); Cand 3–10: group 3 (high salt diet + candesartan cilexetil (3–10 weeks)); Cand 3–16: group 4 (high salt diet + candesartan cilexetil (3–16 weeks)). * $p < 0.05$, ** $p < 0.01$ vs. High group.

interest, the blood pressure of the rats in group 3 (treated with candesartan cilexetil from 3–10 weeks) was also reduced to a value of 153 ± 2 mm Hg at 16 weeks, even though the antihypertensive treatment had already been discontinued for 6 weeks at that time.

Effects of Treatment of Pre-Pubescent Rats with Candesartan Cilexetil on Heart Weight and Aortic Wall Thickness in Dahl-S Rats

Cardiovascular hypertrophy was assessed by measurement of heart weights, and histological assessment of aortic wall thickness. As shown in figure 2, heart weight/body weight ratios were increased in all the high salt diet-treated groups compared to rats on a normal salt diet. The treatments with candesartan cilexetil caused a tendency to decreases in heart weight/body weight ratios, but the changes did not attain statistical significance. A significant increase in aortic wall thickness was also seen in the high salt group (group 2) compared to the normal salt group (group 1). This increase was significantly ($p < 0.05$) attenuated by the rats treated continuously with candesartan cilexetil (group 4), but not in rats treated with prepubertal candesartan cilexetil (group 3).

Effects of Treatment of Pre-Pubescent Rats with Candesartan Cilexetil on Proteinuria and Renal Histology in Dahl-S Rats

As shown in figure 3, the rats on a high salt diet (group 2) had marked proteinuria compared to rats on the normal salt diet at 16 weeks. Examination of urine protein at different time points revealed that the proteinuria developed progressively after starting the high salt diet. At 16 weeks, proteinuria in the rats treated with prepubertal candesartan cilexetil (group 3) was significantly ($p < 0.05$) attenuated. Proteinuria was also decreased in the rats treated continuously with candesartan ($p < 0.01$). Of interest, the changes in the values of plasma total cholesterol (fig. 3c) showed the same trend as the changes in urine protein.

Renal histological changes in the different groups are shown in figure 3d, and representative tissue sections presented in figure 4. High salt treatment caused glomerular sclerosis and vascular hypertrophy. These changes were attenuated, but not completely prevented in the groups treated either prepubertally or continuously with candesartan cilexetil.

Effects of Treatment of Pre-Pubescent Rats with Candesartan Cilexetil on Blood Chemistries, and Renal Renin and AT Receptor Subtype mRNA Expression in Dahl-S Rats

Blood chemistries in the different groups are shown in table 1. No significant differences in blood urea nitrogen, creatinine, total protein, or triglycerides were seen between groups. Plasma renin activity was low (3–5 ng/ml/h) in all groups, and plasma angiotensin II was suppressed to levels below the limit of assay sensitivity.

To further examine changes in the renin-angiotensin system, levels of renin and angiotensin receptor mRNA were examined by semi-quantitiative RT-PCR using our previously described technique [5, 8]. No changes were found in renin, AT1a, AT1b, or AT2 receptor mRNA in the treated and untreated groups (fig. 5, 6).

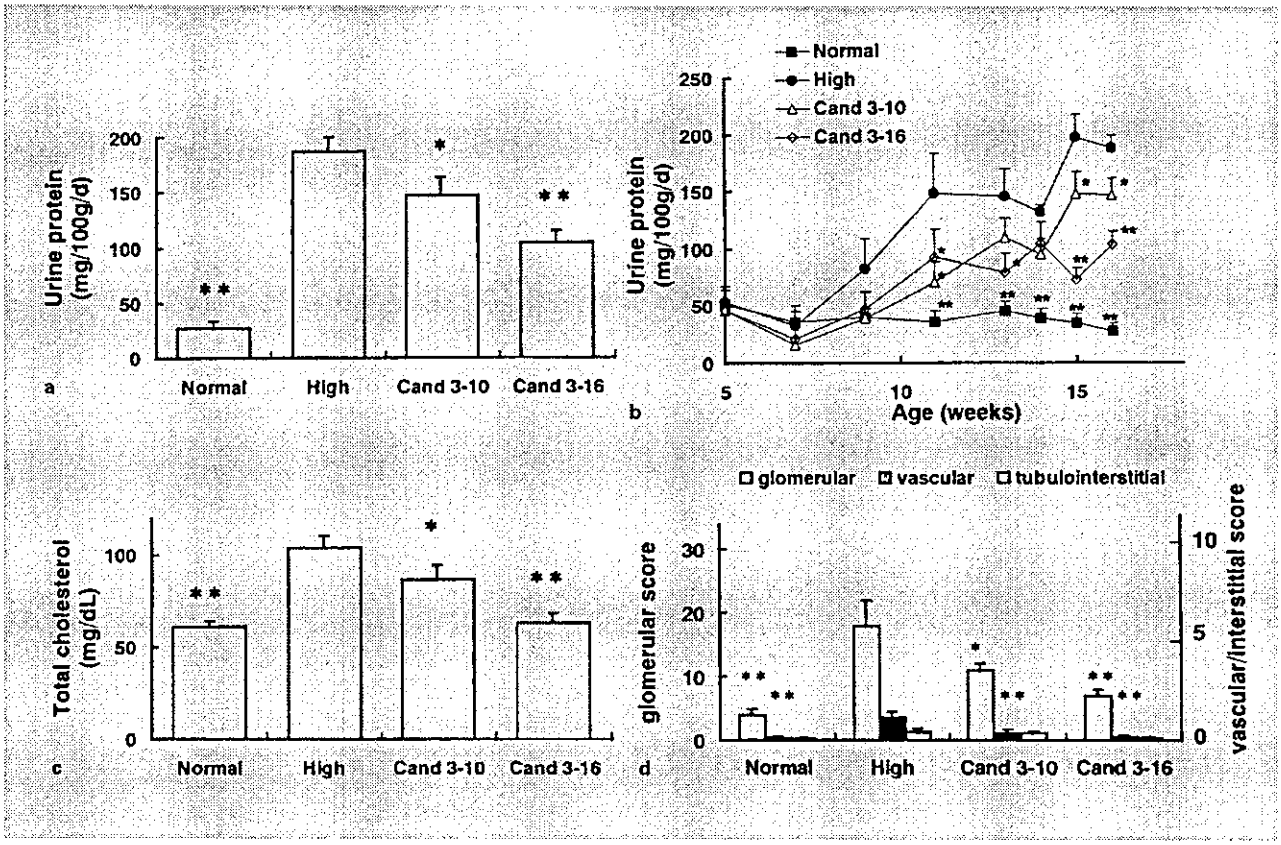

Fig. 3. a Effects of treatment of pre-pubescent rats with candesartan cilexetil (2 mg/kg/d) on urine protein at 16 weeks in Dahl-S rats. **b** Time course of the development of proteinuria in the treated and untreated groups. **c**, **d** Effects of treatment of pre-pubescent rats with candesartan cilexetil (2 mg/kg/d) on **c** plasma total cholesterol and **d** renal histological scoring of glomerular, vascular, and interstitial changes. Normal: group 1 (normal salt diet); High: group 2 (high salt diet); Cand 3–10: group 3 (high salt diet + candesartan cilexetil (3–10 weeks)); Cand 3–16: group 4 (high salt diet + candesartan cilexetil (3–16 weeks)). * $p < 0.05$, ** $p < 0.01$ vs. High group.

Table 1. Blood chemistries and body weights in Dahl-S rats

	Normal (n = 5)	High (n = 5)	Cand 3–10 (n = 6)	Cand 3–16 (n = 5)
Blood urea nitrogen, mg/dl	26±1	24±2	27±3	22±2
Creatinine, mg/dl	0.40±0.02	0.44±0.02	0.48±0.05	0.38±0.02
Total cholesterol, mg/dl	61±10**	104±6	86±8*	63±5**
Triglyceride, mg/dl	70±6	105±22	51±10	94±16
Total protein, g/dl	6.3±0.1	5.8±0.2	6.4±0.1	5.8±0.2
Plasma renin activity, ng/ml/h	3.3±1.2	4.3±0.7	5.0±1.0	3.8±0.4
Plasma angiotensin II, pg/ml	nd	nd	nd	nd
Body weight, g	324±10*	284±10	267±16	300±7

Results shown are the mean ± SEM. * $p < 0.05$; ** $p < 0.01$ vs. High. nd: <3.0 pg/ml.

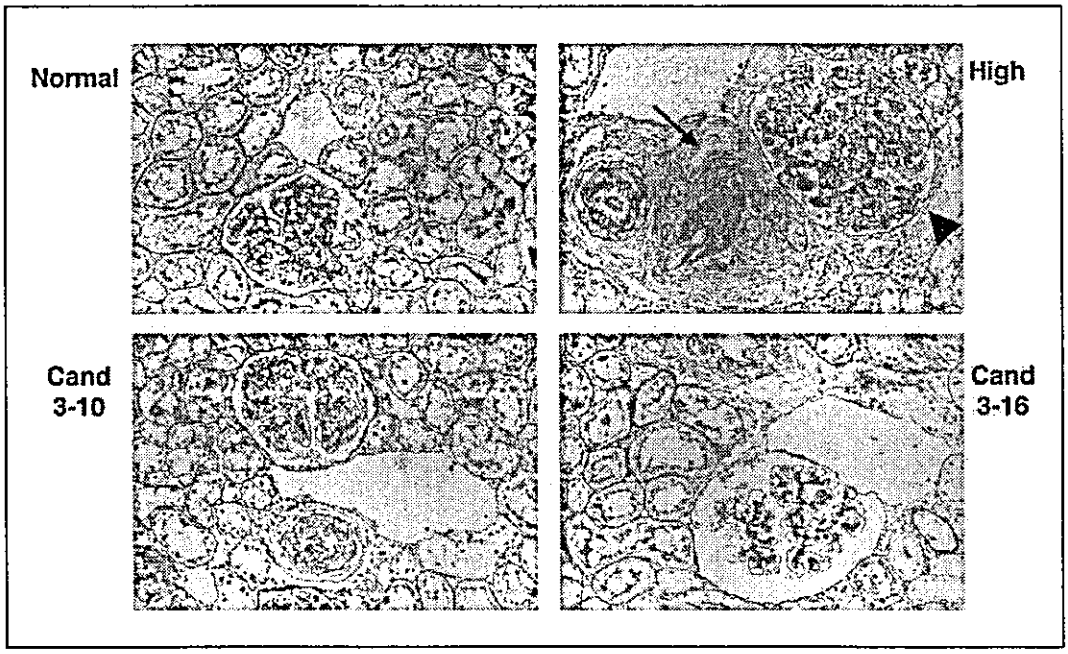

Fig. 4. Light microscopy of renal histology in 16-week-old Dahl-S rats. Representative photomicrographs of formaldehyde-fixed sections stained with PAS are shown. Original magnification × 200. Normal: group 1 (normal salt diet); High: group 2 (high salt diet); Cand 3–10: group 3 (high salt diet + candesartan cilexetil (3–10 weeks)); Cand 3–16: group 4 (high salt diet + candesartan cilexetil (3–16 weeks)). Glomerular changes (arrowhead) and hyperplasia of small to medium sized arteries (arrow) were seen predominantly in the High group.

Discussion

Although there are several rat models for hypertension, the Dahl-S rat was chosen in this study because (1) it has a genetic predisposition to develop hypertension and hypertensive renal damage, (2) the renin-angiotensin system is suppressed in these rats, in contrast to the SHR, where the renin-angiotensin system is elevated, and (3) it may be considered a model of human 'salt-sensitive' hypertension, which may comprise up to one-half of hypertensive patients [9]. We also deliberately chose this model, because it has been reported to be most resistant to the effects of ACEI and ARB, both in terms of the control of

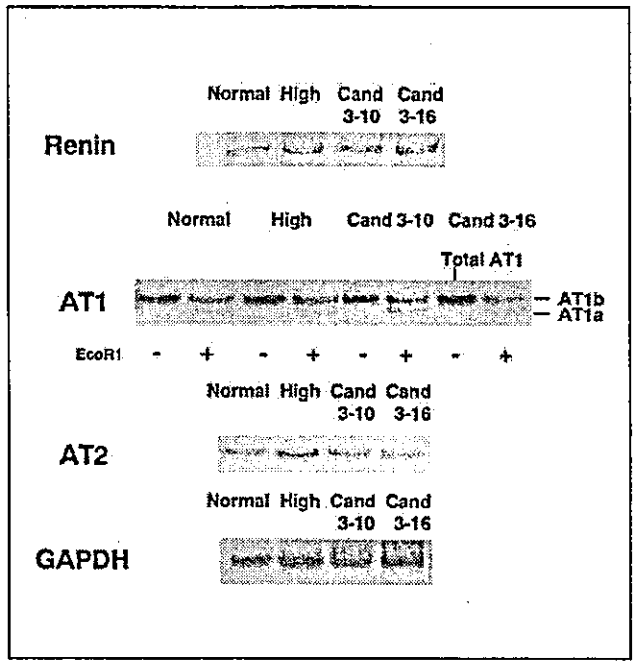

Fig. 5. Representative image of RT-PCR of renin, AT receptor, and GAPDH mRNA in the kidneys of 16-week-old Dahl-S rats. Normal: group 1 (normal salt diet); High: group 2 (high salt diet); Cand 3–10: group 3 (high salt diet + candesartan cilexetil (3–10 weeks)); Cand 3–16: group 4 (high salt diet + candesartan cilexetil (3–16 weeks)).